IEEE Photonics Journal
An IEEE Photonics Society Publication

A Label-Free Optical Biosensor Built on a Low-Cost Polymer Platform

Volume 4, Number 3, June 2012

Linghua Wang
Jun Ren
Xiuyou Han
Tom Claes
Xigao Jian
Peter Bienstman
Roel Baets
Mingshan Zhao
Geert Morthier

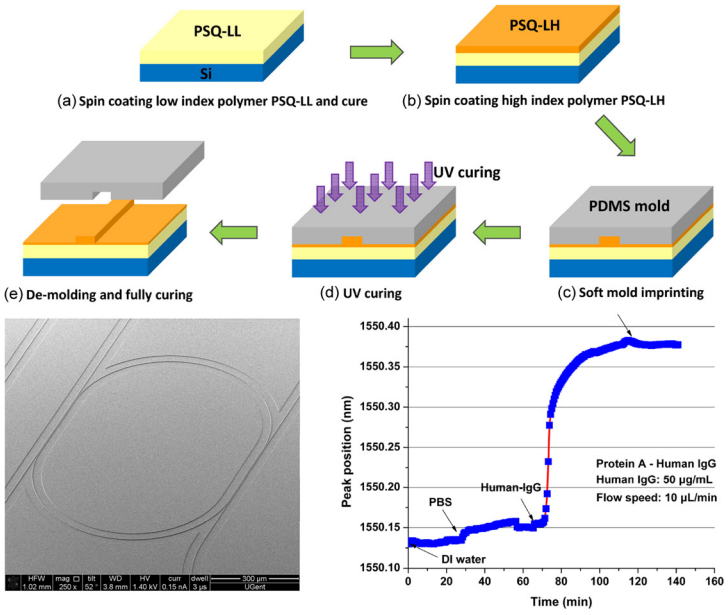

DOI: 10.1109/JPHOT.2012.2200671
1943-0655/$31.00 ©2012 IEEE

IEEE photonics SOCIETY

IEEE

A Label-Free Optical Biosensor Built on a Low-Cost Polymer Platform

Linghua Wang,[1,2,4] Jun Ren,[3] Xiuyou Han,[1] Tom Claes,[2,4] Xigao Jian,[3] Peter Bienstman,[2,4] Roel Baets,[2,4] Mingshan Zhao,[1] and Geert Morthier[2,4]

[1]School of Physics and Optoelectronic Engineering, Dalian University of Technology, 116023 Dalian, China
[2]Photonics Research Group, INTEC-Department, Ghent University-IMEC, 9000 Ghent, Belgium
[3]Faculty of Chemical, Environmental and Biological Science and Technology, Dalian University of Technology, 116023 Dalian, China
[4]Center for Nano- and Biophotonics (NB-Photonics), Ghent University, 9000 Ghent, Belgium

DOI: 10.1109/JPHOT.2012.2200671
1943-0655/$31.00 ©2012 IEEE

Manuscript received April 29, 2012; accepted May 14, 2012. Date of publication May 22, 2012; date of current version May 31, 2012. This work was performed in the context of the Belgian IAP project Photonics@BE. This work is also supported in part by National High-tech R&D Program (No. 2012AA040406) and in part by National Natural Science Foundation of China (No. 60577014, No. 61077015, No. 60807015). Corresponding author: M. Zhao (e-mail: mszhao@dlut.edu.cn).

Abstract: Planar integrated optical biosensors are becoming more and more important as they facilitate label-free and real-time monitoring with high sensitivity. In this paper, the systematic work on the development of this kind of optical biosensor built on a novel polymer platform named PSQ-Ls will be presented. The material itself is of very low cost, and the optical devices with high performances are fabricated through a simple UV-based soft imprint lithography technique. Especially for ring resonator, Q value as high as 5×10^4 and 2.7×10^4 are achieved in air and water condition. These optical chips are functionalized efficiently with protein A molecules through physical immobilization, after careful investigation of the physicochemical and chemical properties of their surface. Both bulk sensing and surface sensing are performed. The proposed optical biosensor exhibits good response not only to its surrounding environment's change but also to the small amount of targeted molecules appearing in the buffered solution, which is human-IgG in our study.

Index Terms: Biosensor, ring resonator, polymer waveguides, imprint lithography.

1. Introduction

Biological and chemical sensors have become more and more important due to their vast application potential in the fields of food safety, environmental monitoring, point-of-care diagnostics, drug discovery and so on. Among different types of sensors, planar integrated photonic biosensors have distinct advantages. Label-free and real-time monitoring of the dynamics of biomolecules' reactions are feasible when an integrated photonic device is used as transducer, avoiding the traditional method of enzyme-linked immunosorbent assay (ELISA), which is labor and time consuming. In addition, these planar photonic biosensors have the capability to be further integrated with other electronic, photonic, biochemical and microfluidic components, thus paving the way toward the realization of "Lab-on-Chip" [1]. One good candidate for this is silicon photonics, which has gained significant progress with vast investment recently. State-of-the-art silicon photonic devices (e.g., microring resonator) has been shown [2], pushing label-free biosensing closer to application level [3]. However, further reducing the cost of these photonic devices would still be desired to make as many users as possible benefit from this technology.

Among different materials, polymer has been proven to be an ideal material option for integrated photonic devices [4], [5]. The cost of the material itself is very low, which makes it attractive where the economic factor needs to be taken into account. The tunable properties of the polymer give the design and fabrication of the photonic devices much more flexibility. Compared to inorganic materials, biocompatiblity is another important and unique feature of polymers. Moreover, the biochemical surface treatment of the polymer photonic devices can be greatly simplified. Also, besides the traditional mature semiconductor processing methods, many novel fabrication techniques, nanoimprint lithography for example, can be applied to process the polymer [6], [7]. The latter method has lots of merits such as high resolution, minimal requirements for complicated equipment, simple fabrication processes involved, and a huge potential for high throughput. Based on the advantages mentioned above, this platform provides us an opportunity to develop an extremely low cost thus disposable label-free optical biosensor.

In this paper, a label-free optical biosensor built on a low-cost polymer platform will be presented. First, a simple and fast fabrication process utilizing the UV-based soft imprint lithography technique is discussed. No extra specific imprint equipment, which is normally expensive, is required during the imprinting process. After solving two problems, residual layer thickness and surface smoothness, which are usually parasitic with the soft imprint lithography, we obtain a high quality ridge shape waveguide. Then the technique is applied to fabricate a laterally coupled optical microring resonator. This kind of resonant structure is attractive for biosensing because it effectively increases the interaction length between the evanescent field of the waveguide mode and the target analyte without increasing the physical length of the sensing arm, thus reducing the device's footprint. With the improvement of the fabrication technique, we achieve high quality factors for the microring resonator both in air and in water, of around 5×10^4 and 2.7×10^4, respectively. These values are among the highest values reported so far for polymer-based microring resonators. With the solution delivering capability provided by the microfluidic channel that is assembled with the device chip, the results for the homogeneous sensing of NaCl solutions under different concentrations are presented. Sensitivity of 50 nm/RIU with good linearity is obtained. In the next step, in order to demonstrate sensing of biomolecules, the surface of the microring resonator is functionalized with bioreceptor protein A to provide binding sites for its affinity pair human-IgG. Compared with the multistep chemical surface treatment commonly adopted on inorganic-based optical devices, our method takes advantage of the biocompatibility of the polymer material itself, and is much more simple and efficient. The details of the surface treatment procedures and their characterization will be revealed. Finally, the measurement results on the surface sensing caused by binding events of human-IgG and protein A on the optical biosensor will be presented.

2. Waveguide Materials

The polymer material used for the fabrication of the optical waveguide should meet certain requirements such as optical properties, thermal stability and so on. In order to utilize UV-based soft imprint lithography, it has to be UV curable and preferably not very viscous. For the biosensing application, the polymer also needs to be stable within the surface treatment and measurement environment.

The polymer we use in this work is a silicate-based inorganic-organic hybrid polymer named PSQ-Ls, which can meet most of the requirements mentioned above [8], [9]. The material not only has good optical properties such as low optical loss at the telecommunication wavelengths (< 0.3 dB/cm at 1310 nm, < 0.9 dB/cm at 1550 nm), high thermal stability (1% Td is above 300 °C in air and 340 °C in nitrogen) but more importantly, its pure liquid (solvent-free) and UV curable property makes it highly compatible with the developed UV-based soft imprint lithography. The material has two components, PSQ-LH with high refractive index $(n = 1.52)$ and PSQ-LL with low refractive index $(n = 1.45)$, which are used as the waveguide core and bottom cladding, respectively. Its good material stability will be proved later in the subsequent surface binding sensing experiment.

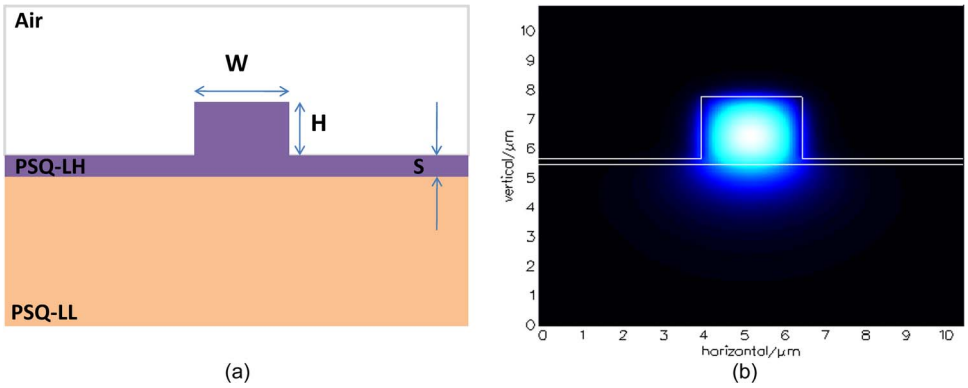

Fig. 1. (a) The schematic picture of the proposed ridge shaped waveguide. (b) The simulated fundamental TE mode of the waveguide.

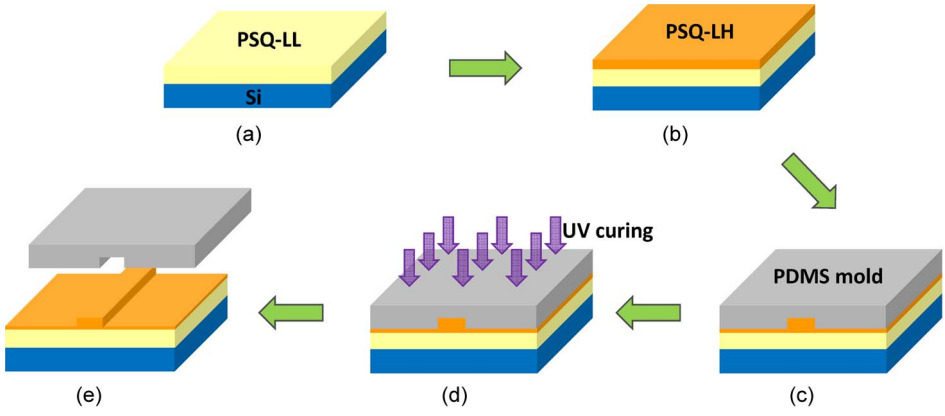

Fig. 2. Fabrication process of the UV-based soft imprint lithography. (a) Spin coating low index polymer PSQ-LL and cure. (b) Spin coating high index polymer PSQ-LH. (c) Soft mold imprinting. (d) UV curing. (e) De-molding and fully curing.

3. Waveguide Design Considerations and Fabrication

In our previous work, we demonstrated the design and fabrication of an inverted-rib polymer waveguide [10]. This type of waveguide has the advantages of low loss, easy fabrication and good tolerance to the slab waveguide height, and is suitable for constructing passive devices such as Y splitters and notch filters. However, due to the high index contrast between the waveguide core and air (upper cladding), most of the light is confined within the waveguide core and lower cladding. Only a small portion of the light is able to penetrate into the upper cladding to interact with the analyte, thus making it unsuitable for biosensing applications. In that case a ridge shape waveguide structure is preferred. Fig. 1(a) gives the schematic picture of the waveguide cross section we propose this time for the biosensing application. The designed values for the waveguide width W, waveguide height H and residual slab waveguide height S are 2.5 μm, 2.1 μm and 0.2 μm, respectively. The corresponding TE mode field calculation is shown in Fig. 1(b). These values are chosen according to the considerations of the waveguide sensitivity, bending and radiation loss as well as the fabrication process. The residual slab waveguide on either side of the core is a special issue that needs to be dealt with, which will be discussed in detail below.

Simplicity without resorting to expensive equipment is the one of the most attractive advantages of UV-based soft imprint lithography technique. The fabrication process we developed is shown in Fig. 2, which involves only a few steps. First, the polymer material with lower refractive index named PSQ-LL is spin-coated on a silicon substrate and fully cured to act as the waveguide bottom

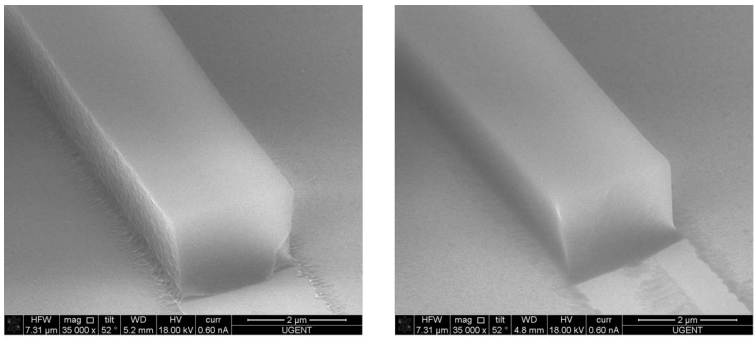

(a) (b)

Fig. 3. Reduction of the surface roughness of the master mold (a) before and (b) after the thermal flow treatment.

cladding. The thickness is controlled to be over 6 μm to prevent substrate leakage loss. Second, the core layer material PSQ-LH is spin coated with the speed of 6000 rpm for 40s to form a layer of 2 μm. After that, the prepared soft Polydimethylsiloxane (PDMS) mold with the waveguide patterns on it is used to imprint this layer. During this process, special attention has to be paid to prevent inducing trapping of air bubbles between the mold and the substrate. Because of the softness of the mold, it is easy to make the center area of the mold to bow outwards to contact with the core layer first, then slowly lower down the remaining part of the imprinting mold. In this way, the trapped air bubble can be squeezed out along the waveguide pattern, making the waveguide patterns void free. Around 3 min of UV illumination with an intensity of 30 mW/cm^2 in nitrogen atmosphere is used to UV cure the waveguide core layer. The waveguide patterns can be shaped with good conformity to those on the mold, which can be easily detached from the substrate because of the hydrophobic property of the mold. Finally, post baking at 180 °C for 2 hours and 200 °C for another 2 hours allows full polymerization of the waveguide core layer.

Two important issues need to be addressed properly during the fabrication process: the waveguide roughness and the residual slab waveguide thickness. The soft mold we use for imprinting is replicated from a SU-8 master mold by the cast-molding method. Compared with the master mold made by dry etching [11], [12], in silicon or silica for example, the SU-8 mold can be obtained from a standard lithography process, which is more easy, reliable and repeatable. Moreover, the master mold made in this material leaves more room for improving the surface smoothness of the defined patterns. By post thermal flow treatment at 180 °C for 3 minutes after developing, the roughness of the surfaces of the waveguide is greatly reduced. The experimental results are shown in Fig. 3.

Another problem that needs to be tackled properly is how to reduce the residual slab waveguide thickness, which is a tough issue especially for soft imprint lithography. This residual layer on both sides of the waveguide core left by imprinting can result in high radiation loss, preventing the waveguide to be bent into compact structures such as rings with small radii. Other researchers have spent a lot of effort to solve it, but usually the proposed solutions require expensive imprinting equipment or a specific setup, the vacuum-assisted microfluidic technique for example in [13]. In the past we circumvented this problem by adopting an inverted rib shape waveguide and obtained a high Q-factor microring resonator [10]. The method proved to be effective for fabricating passive waveguide devices. However, as explained before, a ridge shaped waveguide structure is preferred for biosensing applications. In order to achieve that, we adopt an innovative "minimum polymer squeezing" method. The ridge shape waveguide is obtained by imprinting two trenches on both sides of the waveguide, instead of using the single trench pattern on the mold to directly imprint the waveguide in the core layer. A schematic picture is shown in Fig. 4. The advantage of this method is that the resistance of the polymer against the mold is low because only a small amount of the polymer needs to be squeezed by the mold, thus the requirement for the strength of the forces exerted on the mold is greatly minimized. No additional imprinting tool is used during the imprinting

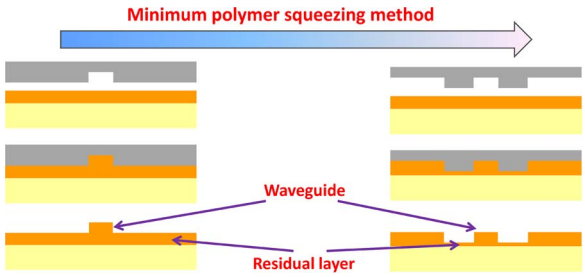

Fig. 4. Schematic picture of the "Minimum polymer squeezing method" for the reduction of the residual layer on the sides of the ridge waveguide.

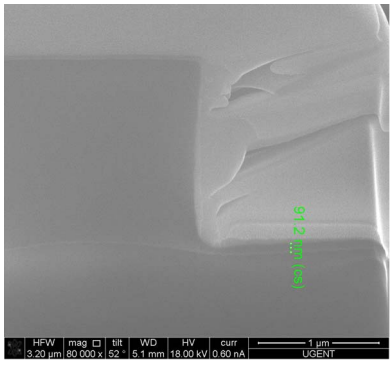

Fig. 5. SEM picture of the fabricated ridge shape waveguide with negligible residual layer thickness.

process, in which the polymer waveguide is patterned only by the capillary forces between the PDMS soft mold and the substrate. A polymer waveguide with good rectangular shape as well as negligible residual layer thickness (below 100 nm) fabricated with this method is shown in Fig. 5. A similar strategy was used by T. Han etc. in [14] to obtain a low loss straight waveguide. Considering both the ease of polymer material synthesis and the simple fabrication process, this technique holds the promise for fabricating different kinds of polymer-based photonic devices at a very low cost, including an optical biosensor.

4. Design of the Microring Resonator

The microring resonator has become an attractive candidate for functioning as transducer of label-free optical biosensors recently [15]–[19]. Due to the resonant cavity enhancement effect, the interaction length between the optical waveguide mode and its surrounding environments is increased while keeping the device's size as compact as possible. In this paper, a laterally coupled racetrack resonator is chosen as one step of imprinting is enough to pattern the structure. Several critical parameters are carefully chosen to optimize the performances of the device which is used as optical biosensor. For example, the radius of the ring is set to be 350 μm, which is closely related to its free spectral range (FSR). Too small FSR will result in an insufficient dynamic range, while too large FSR increases the sweeping time step between two consecutive measurements during the time monitoring. The gap and coupling length between the straight waveguide and the ring resonator are designed to be 1 μm and 70 μm, respectively. The weak coupling between them guarantee that the resonator can still maintain good performance in aqueous environment despite of the higher losses brought by the absorption of the water as well as the relatively increasing coupling efficiency compared with that in air. The SEM pictures of the devices obtained by the UV-based soft imprint lithography are shown in Fig. 6. The transmission spectrum of the fabricated device measured both in air and water conditions are shown in Fig. 7, in which the fitting results are

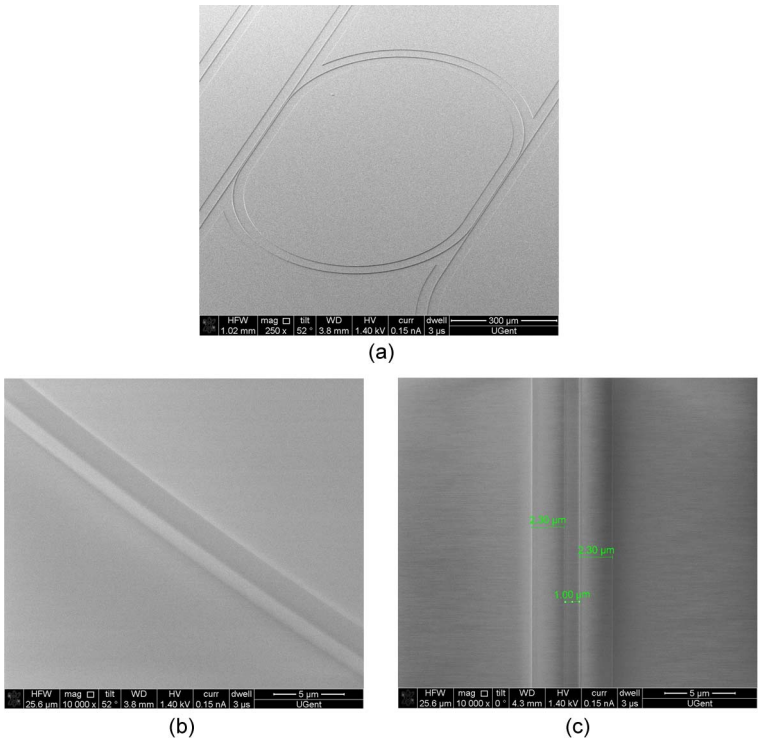

Fig. 6. SEM pictures of the ring resonator fabricated by UV based soft imprint lithography technique. (a) Image of the entire structure. (b) Port waveguide. (c) Detail of the coupling region.

also presented. The good properties of the device prove the effectiveness of the fabricating procedures aiming to improve the quality of the polymer waveguide. The high Q factor, 5×10^4 and 2.7×10^4 in two cases, are among the highest values reported so far for polymer-based microring resonators, which is also a good criteria for optical biosensor since it is in inversely proportional relationship with optical biosensor' s detection limit.

5. Microfluidics Channel

A promising way to bond the transducer chip to a fluidics channel is developed with the flip-chip equipment. With the "stamp-and-stick" method [20], the PDMS fluidics channel is mounted on top of the chip with ring resonators on it. The test solution can be delivered to the ring via inlet and outlet microtubes with a syringe and syringe pump. A reliability test is done to test the bonding property to prevent possible leakage.

6. Bulk Sensing

To demonstrate bulk sensing, a NaCl solution is chosen as the analyte to flow over the ring resonator through the fluidics channel, which serves as upper cladding of the ring resonator. The refractive index of this upper cladding is modified by the NaCl, which in turn changes the effective refractive index of the guided mode of the ring resonator and thus its resonant wavelength. The measurement result is shown in Fig. 8, where the correspondence between NaCl concentrations and refractive index changes is made using the equation proposed in [21]. As expected, a higher NaCl concentration causes larger refractive index change thus resulting in larger resonant wavelength shift. The good linearity relationship also proves the stability of this kind of polymer during working in NaCl solution. Around 50 nm/RIU sensitivity is obtained, slightly less than the 70 nm/RIU sensitivity achieved in [15] with a silicon microring resonator. This is due to the low refractive index of polymer itself, which can be improved with novel nanoporous polymer as reported in [22]. However, because

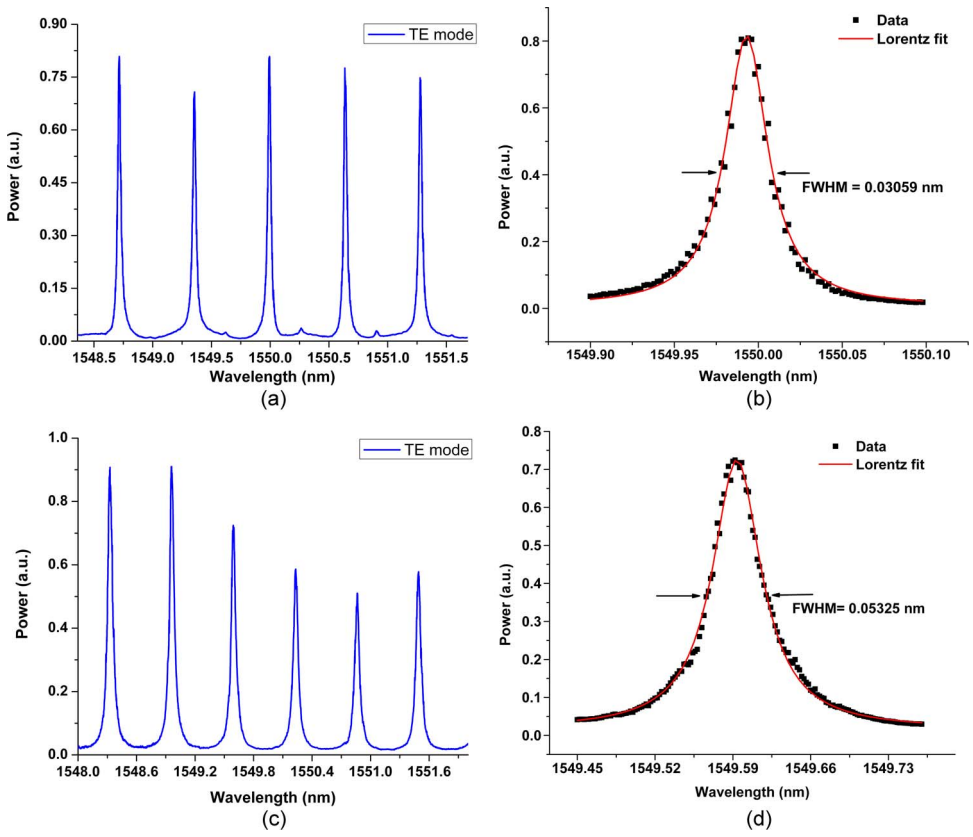

Fig. 7. Measuring results of the fabricated ring resonator with (a) Air as upper cladding, (b) Fitting result of (a), (c) Water as upper cladding, (d) Fitting result for (c).

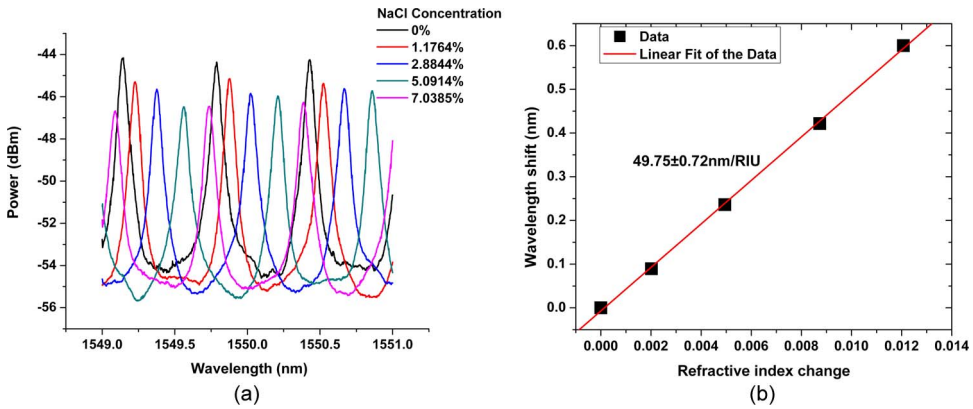

Fig. 8. Spectral shift of the microring resonances when flowed with NaCl solutions with different concentrations. (a) Change of the spectrum at the drop port. (b) Resonant peak positions and their linear fit.

of the small width of the resonance achieved in Fig. 7(d), a refractive index change down to10^{-5} can still be detectable considering the 3σ noise level of around 3 pm [23].

7. Surface Sensing

As a first step toward specific antigen-antibody sensing, we demonstrate sensing of surface binding here. To this end, the waveguide surface needs to be treated to have receptors with binding sites

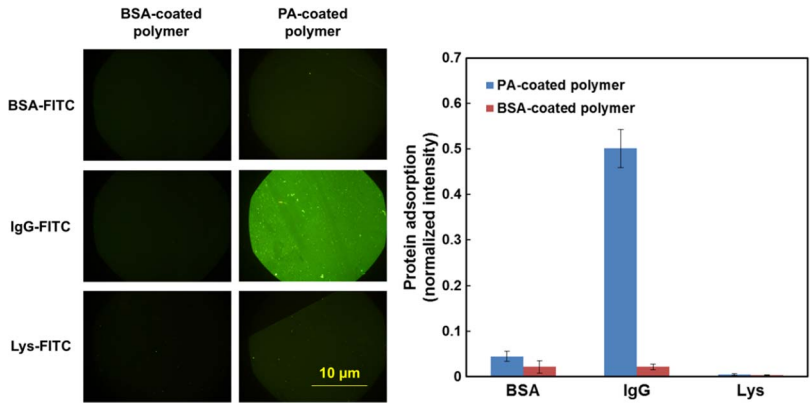

Fig. 9. Selective adsorption of IgG on PA-coated polymer surface. PA-coated polymer slides (right line) and BSA-coated polymer slides (left line) were incubated with BSA-FITC, IgG-FITC and Lys-FITC conjugate solutions for 10 min at room temperature. All fluorescence micrographs were taken under identical conditions: Magnification 100×, exposure time 1/7 s. The fluorescence intensity of each image was analyzed quantitatively and normalized by removing the effect of fluorescence background and considering the individual F/P mass ratio of each protein, which allow a direct comparison of coupling amount between different proteins.

immobilized on it. In this paper, IgG (human Immunoglobulin G) and PA (Staphylococcal protein A) are chosen as an affinity model. Antibody research is of high importance in life sciences because of its unique capability of identifying and neutralizing foreign objects such as bacteria and viruses. High affinity of IgG toward protein A but with moderate dissociation constant $(10^{-6}$ M) makes it a much more representative model than the widely used biotin-avidin one, whose dissociation constant is as high as 10^{-15} M.

7.1. Loading of Receptor Proteins on the Surface of Polymer Chips

Protein immobilization strategies for biochips involve physical and covalent methods, and the choice of a suitable one is primarily determined by the physicochemical and chemical properties of the interface. Covalent immobilization of bio-receptors on optical biosensors built on inorganic platforms, silicon-on-insulator (SOI) for example, have already been demonstrated, where the typical multistep reactions include surface activation, silanization, target molecule coupling and blocking [24]. This method is not only time and labor consuming, but more importantly, it is a big question whether the polymer-based optical devices can withstand the multistep chemical treatments during this process and can still be stable in measurement environment after that. Compared to that, physical immobilization via direct incubation is much more appropriate for polymer-based optical chips. Generally, proteins can be adsorbed on chip surfaces via intermolecular forces, mainly with ionic bonds and hydrophobic interactions [25], [26]. Our research found that the silicate-based inorganic-organic hybrid polymer waveguide material we used in this work shows a moderate hydrophobicity with the water contact angle of 97°. Such a hydrophobic extent could provide a necessary binding strength, which facilitates stable attachment between material surface and a majority of proteins. At the same time, the hydrophobicity is not so high as to essentially affect the conformation and function of the retained proteins. Under physiological solution conditions (0.01 M PBS, pH 7.4, containing 0.154 M NaCl), PA molecules were coated on the surface of polymer slides effectively through an incubation process. Further characterization with a fluorescence analysis found that the resultant PA-coated chip had a good performance in binding its affinity target, human-IgG, while its binding capacities toward two other proteins, BSA and Lysozyme, were not significant compared to the control that employ BSA as immobilized protein. The results are shown in Fig. 9, which indicated that immobilization of PA did not lead to significant loss of IgG-binding activity. More important, since PA has a relatively small molecular size and a less complex spatial structure, the protein layer had a good coverage on the surface of the polymer. Thus, the surface area that could accommodate other proteins and result in

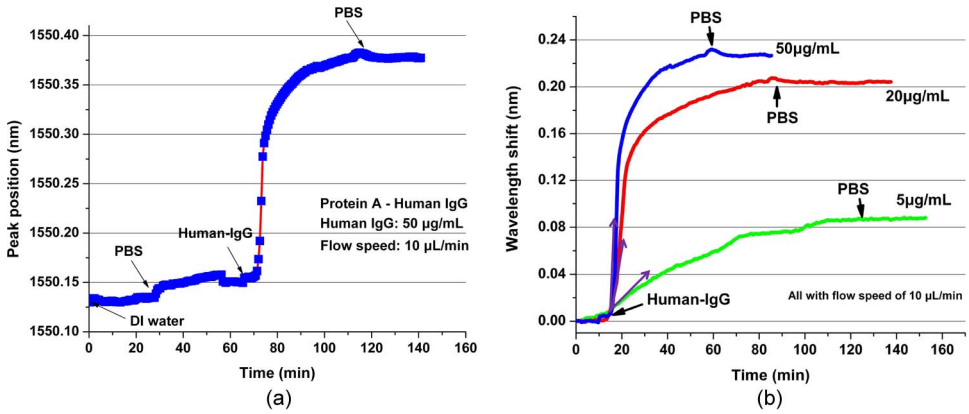

Fig. 10. (a) The entire monitoring process for the surface sensing with protein A as bioreceptors immobilized on the chip surface. (b) The responsivities of the optical biosensors toward different antibody's concentrations.

nonselective adsorption was limited. Therefore, surface functionalization through physical immobilization has been proved to be effective enough for the fabricated optical chip. Its good perfomance on PA coupling makes it a good alternative for antibody oriented immobilization.

7.2. Surface Binding Sensing Measurement Results

Deionized (DI) water, 0.01 $\times$ Phosphate Buffer Solution (PBS), Human-IgG with a concentration of 50 μg/ml and 0.01 $\times$ PBS are pumped into the fluidics channel consecutively, all with the flow speed of 10 μL/min. The resonant peak position, which is determined by the Lorentz fitting, is recorded as a function of the time during the process. The measurement result is shown in Fig. 10(a). As can be seen from that, the proposed polymer-based optical biosensor is stable in the measurement environments, with almost zero wavelength shift in DI water in the first phase and only around 10 pm wavelength shift in PBS in the second phase. This is probably due to the ion incorporation on the functionalized surface of the polymer waveguide. It is a small enough value if compared with the dramatic wavelength shift in the third phase, where the nearly 230 pm change is caused by the affinity of human-IgG to the protein A molecules that are immobilized on the chip surface as bio-receptors. No obvious reverse wavelength shift is observed in the last phase of PBS rinsing, which indicates the strong binding strength between the protein A and human-IgG. It is also a proof that coating of protein A to the chip surface is successful. Finally, the biosensors working under different concentrations of Human-IgG solutions are tested. As can be seen in Fig. 10(b), the optical biosensors exhibit different dynamic responsivities toward the antibody's concentrations. So far, the human-IgG with concentration down to 5 μg/ml can be easily detected as the signal is still significantly above the noise level. Detection with even lower antibody's concentration can be expected.

Incorporation of polymer-based surface grating coupler with the biosensor enables easy alignment and multiplexed sensing [27]. Cheap sources and detectors can be utilized if working wavelength is shifted to shorter band (e.g., visible wavelength), which is feasible for polymer waveguide biosensor. Athermal polymer microring resonator can be designed and fabricated to eliminate the temperature noise during biosensing. These aspects are going to be further improved in our next step.

8. Conclusion

In summary, we develop a rather simple UV-based soft imprint technique using a novel polysiloxane liquid optical material named PSQ-Ls. Photonic devices can be obtained with one step imprinting. Based on this, ring resonator with very high Q value is obtained, which is then used as optical biosensor. The bulk sensing experiment with NaCl solutions shows a sensitivity of 49.75 nm/RIU. After investigation of the physicochemical and chemical properties of the interface, a simple but

efficient method to immobilize the bio-receptors onto the surface of the optical chip, which is protein A in our case, is developed. Surface binding sensing is demonstrated with protein A's affinity pair, human-IgG. Our study confirms the possibility that polymer-based optical biosensors with surface functionality can perform well in aqueous environment. Considering the constituents that are included within this work, ranging from material, fabrication technique to surface functionalization method, a very low cost optical biosensor built on a polymer platform is promising, which would find vast applications in the fields of environmental monitoring, food safety, and diagnostic applications.

Acknowledgment

The authors would like to thank Steven Verstuyft and Liesbet Van Landschoot's help on the fabrication and characterization. Linghua Wang acknowledges CSC scholarship and Ghent University BOF co-funding for financial support.

References

[1] X. Fan, I. M. White, S. I. Shopoua, H. Zhu, J. D. Suter, and Y. Sun, "Sensitive optical biosensors for unlabeled targets: A review," *Anal. Chim. Acta*., vol. 620, no. 1/2, pp. 8–26, Jul. 2008.
[2] W. Bogaerts, P. De Heyn, T. Van Vaerenbergh, K. De Vos, S. Selvaraja, T. Claes, P. Dumon, P. Bienstman, D. Van Thourhout, and R. Baets, "Silicon microring resonators," *Laser Photon. Rev*., vol. 6, no. 1, pp. 47–73, 2012.
[3] M. Iqbal, M. A. Gleeson, B. Spaugh, F. Tybor, W. G. Gunn, M. Hochberg, T. Baehr-Jones, R. C. Bailey, and L. C. Gunn, "Label-free biosensor arrays based on silicon ring resonators and high-speed optical scanning instrumentation," *IEEE J. Sel. Top. Quantum Electron*., vol. 16, no. 3, pp. 654–661, May/Jun. 2010.
[4] H. Ma, A. K.-Y. Jen, and L. R. Dalton, "Polymer-based optical waveguides- materials, processing, and devices," *Adv. Mater*., vol. 14, no. 19, pp. 1339–1365, Oct. 2002.
[5] L. Eldada, "Advances in polymer-based dynamic photonic components, modules, and subsystems," *Proc. SPIE*, vol. 6351, pp. 63510Y-1–63510Y-10, 2006.
[6] L. J. Guo, "Nanoimprint lithography: Methods and material requirements," *Adv. Mater*., vol. 19, no. 4, pp. 495–513, Feb. 2007.
[7] J. K. S. Poon, Y. Y. Huang, G. T. Paloczi, and A. Yariv, "Soft lithography replica molding of critically coupled polymer microring resonators," *IEEE Photon. Technol. Lett*., vol. 16, no. 11, pp. 2496–2498, Nov. 2004.
[8] H. B. Zhang, J. Y. Wang, L. K. Li, Y. Song, M. S. Zhao, and X. G. Jian, "A study on liquid hybrid material for waveguides—Synthesis and property of PSQ-Ls for waveguides," *J. Macromol. Sci., Pure Appl. Chem*., vol. 45, no. 3, pp. 232–237, 2008.
[9] X. Han, L. Wang, Y. Liu, H. Zhang, J. Wang, X. Jian, and M. Zhao, "Properties of liquid inorganic-organic hybrid polymer optical waveguide materials," *Proc. SPIE*, vol. 7134, pp. 713416-1–713416-10, 2008.
[10] J. Teng, S. Scheerlinck, H. Zhang, X. Jian, G. Morthier, R. Beats, X. Han, and M. Zhao, "A PSQ-L polymer microring resonator fabricated by a simple UV-based soft-lithography process," *IEEE Photon. Technol. Lett*., vol. 21, no. 18, pp. 1323–1325, Sep. 2009.
[11] C.-H. Lin and R. Chen, "New approaches of mold fabrication for nanoimprint lithography," *J. Micro/Nanolith. MEMS MOEMS*, vol. 10, no. 1, pp. 011506-1–011506-6, Jan.–Mar. 2011.
[12] S. H. Oh, S. Uk Cho, C. S. Kim, Y. G. Han, C.-S. Cho, and M. Y. Jeong, "Fabrication of nickel stamp with improved sidewall roughness for optical devices," *Microelectron. Eng*., vol. 88, no. 9, pp. 2900–2907, Sep. 2011.
[13] A. Flores, S. Song, S. Baig, and M. R. Wang, "Vacuum-assisted microfluidic technique for fabrication of guided wave devices," *IEEE Photon. Technol. Lett*., vol. 20, no. 14, pp. 1246–1248, Jul. 2008.
[14] T. Han, S. Madden, M. Zhang, R. Charters, and B. Luther-Davies, "Low loss high index contrast nanoimprinted polysiloxane waveguides," *Opt. Exp*., vol. 17, no. 4, pp. 2623–2630, Feb. 2009.
[15] K. De Vos, I. Bartolozzi, E. Schacht, P. Bienstman, and R. Baets, "Silicon-on-insulator microring resonator for sensitive and label-free biosensing," *Opt. Exp*., vol. 15, no. 12, pp. 7610–7615, Jun. 2007.
[16] J. B. Wright, I. Brener, K. R. Westlake, D. W. Branch, M. J. Shaw, and G. A. Vawter, "A platform for multiplexed sensing of biomolecules using high-Q microring resonator arrays with differential readout and integrated microfluidics," *Proc. SPIE*., vol. 7605, p. 76050C1-11, 2010.
[17] T. Claes, W. Bogaerts, and P. Bienstman, "Experimental characterization of a silicon photonic biosensor consisting of two cascaded ring resonators based on the Vernier-effect and introduction of a curve fitting method for an improved detection limit," *Opt. Exp*., vol. 18, no. 22, pp. 22 747–22 761, Oct. 2010.
[18] A. Ramachandran, S. Wang, J. Clarke, S. J. Ja, D. Goad, L. Wald, E. M. Flood, E. Knobbe, J. V. Hryniewicz, S. T. Chu, D. Gill, W. Chen, O. King, and B. E. Little, "A universal biosensing platform based on optical micro-ring resonators," *Biosens. Bioelectron*., vol. 23, no. 7, pp. 939–944, Feb. 2008.
[19] A. Yalcin, K. C. Popat, J. C. Aldridge, T. A. Desai, J. Hryniewicz, N. Chbouki, B. E. Little, O. King, V. Van, S. Chu, D. Gill, M. Anthes-Washburn, M. S. Unlu, and B. B. Goldberg, "Optical sensing of biomolecules using microring resonators," *IEEE J. Sel. Topics Quantum Electron*., vol. 12, no. 1, pp. 148–155, Jan./Feb. 2006.
[20] S. Satyanarayana, R. N. Karnik, and A. Majumdar, "Stamp-and-stick room-temperature bonding technique for microdevices," *IEEE J. Microelectromech. Syst*., vol. 14, no. 2, pp. 392–399, Apr. 2005.

[21] H. Su and X. G. Huang, "Fresnel-reflection-based fiber sensor for on-line measurement of solute concentration in solutions," *Sens. Actuators B, Chem.*, vol. 126, no. 2, pp. 579–582, Oct. 2007.
[22] M. Mancuso, J. M. Goddard, and D. Erickson, "Nanoporous polymer ring resonators for biosensing," *Opt. Exp.*, vol. 20, no. 1, pp. 245–255, Jan. 2012.
[23] I. M. White and X. Fan, "On the performance quantification of resonant refractive index sensors," *Opt. Exp.*, vol. 16, no. 2, pp. 1020–1028, Jan. 2008.
[24] K. De Vos, J. Girones, S. Popelka, E. Schacht, R. Baets, and P. Bienstman, "SOI optical microring resonator with poly(ethyleneglycol) polymer brush for label-free biosensor applications," *Biosens. Bioelectron.*, vol. 24, no. 8, pp. 2528–2533, Apr. 2009.
[25] S. L. Hirsh, M. M. Bilek, N. J. Nosworthy, A. Kondyurin, C. G. dos Remedios, and D. R. McKenzie, "A comparison of covalent immobilization and physical adsorption of a cellulase enzyme mixture," *Langmuir*, vol. 26, no. 17, pp. 14380–14388, Sep. 2010.
[26] F. Rusmini, Z. Zhong, and J. Feijen, "Protein immobilization strategies for protein biochips," *Biomacromol.*, vol. 8, no. 6, pp. 1775–1789, Jun. 2007.
[27] L. Wang, Y. Li, M. Garcia Porcel, D. Vermeulen, X. Han, J. Wang, X. Jian, M. Zhao, and G. Morthier, "Grating couplers in polymer with a thin Si_3N_4 layer embedded," *Proc. SPIE*, vol. 8258, pp. 825817-1–825817-7, 2012.